Reviewed Preprint
v1 • January 16, 2025
Not revised

Reviewed Preprint
v2 • March 12, 2026
Revised by authors

For correspondence:
C.Dekker@tudelft.nl

# equal contribution

Competing interests: No competing interests declared

Funding: See page 12

Reviewing editor: Felix Campelo, Universitat Pompeu Fabra, Spain

Interaction hierarchy among Cdv proteins drives recruitment to membrane necks

Nicola De Franceschi[1,2,#], Alberto Blanch-Jover[1,#], Cees Dekker[1]

[1]Department of Bionanoscience, Kavli Institute of Nanoscience Delft, Delft University of Technology, Delft, Netherlands • [2]IMol Polish Academy of Sciences, Warsaw, Poland

eLife Assessment

This **important** study investigates how the Cdv division proteins of Metallosphaera sedula assemble on and interact with curved membranes in vitro, advancing our understanding of this reduced ESCRT-like machinery. The data provide support for sequential protein recruitment and curvature-dependent enrichment at membrane necks, based on well-controlled reconstitution assays and quantitative analysis. The work establishes a **convincing** experimental framework for dissecting Cdv-mediated membrane remodeling. The study will be of broad interest to evolutionary and synthetic biologists as well as membrane biophysicists.

https://doi.org/10.7554/eLife.104226.2.sa4

Abstract

Cell division in the crenarchaea is accomplished by the Cdv system. In Sulfolobus cells, it was observed that an initial non-contractile ring of CdvA and CdvB forms at the mid location of the cell, which is followed by a second ring of CdvB1 and CdvB2 that appear to drive the constriction of the cell membrane. Here, we use an *in vitro* reconstituted system to explore how protein interactions among these Cdv proteins govern their recruitment to the membrane. We show that CdvA can bind to lipid membranes, but does so more efficiently when it is in complex with CdvB. We find that CdvB2 can polymerize if its self-inhibitory domain is removed, and that by itself is exhibits poor binding to the membrane. However, CdvB2 can be efficiently recruited to the membrane by both CdvB1 and CdvB. Furthermore, the CdvB1:CdvB2 co-polymer can be recruited to the membrane by CdvA:CdvB. By reconstituting these proteins in dumbbell-shaped liposomes, we show that Cdv proteins have a strong preference to localize at membrane necks of high curvature. Our findings clarify many of the mutual protein interactions of the Cdv system and their interaction with the membrane, thus helping to build a mechanistic understanding of cell division in archaeal cells.

Introduction

Cell division in the archaeal phylum of the crenarchaea is performed by the Cdv system (Lindås et al., 2008; Samson et al., 2008). While this protein machinery is unique to archaea, some of its components are homologous to the ESCRT-III proteins that are responsible for the cell division, vesicle budding, and many other reverse-topology membrane-scission processes in eukaryotes (Schöneberg et al., 2017; Hurley, 2015). This homology is one of the many similarities that eukaryotes share with archaea, which reinforces the widespread idea that these two kingdoms of life share an evolutionary root (Cox et al., 2008).

Since the Cdv system was first described 15 years ago in Sulfolobus sulfataricus, it has been shown to be present in many other species of the TACK superphylum of archaea (Makarova et al., 2010). It is composed of CdvA, the CdvB paralogs (homologous to ESCRT-III in eukaryotes), and CdvC

(homologous to the eukaryotic Vps4) (Samson et al., 2008). The first cell imaging of the Cdv system showed a ring of CdvA and CdvB forming at the center of the cell between two segregated nucleoids during division, which over time colocalized with a ring of CdvC in the same position (Lindås et al., 2008). All these 3 proteins are located in the same operon (Lindås et al., 2008), while paralogs of CdvB (namely CdvB1, CdvB2 and CdvB3) are located in other parts of the genome. Recently, it was reported that these paralogs play a crucial role in cell division (Tarrason Risa et al., 2020). A recent model for cell division in crenarchaea is that CdvA and CdvB initially form a ring at the centre of the cell, where it subsequently recruits CdvB1 and CdvB2 (Tarrason Risa et al., 2020). At this point, CdvB is digested by the proteasome and the initial CdvA:CdvB ring gets removed from the membrane, while CdvB1 and CdvB2 are left to perform the constriction of the membrane, presumably through the interaction of CdvB1 directly with the membrane (Blanch Jover et al., 2022), until the final step of scission (Tarrason Risa et al., 2020). CdvC is a AAA ATPase that has been suggested to remove monomers of CdvB1 and CdvB2 from the ring, generating a turnover that ensures cellular constriction while avoiding steric hindrance at the neck (Tarrason Risa et al., 2020; Harker-Kirschneck et al., 2022). This model of action of the Cdv proteins is supported by some experimental findings on live cells. When generating mutant cells of S. sulfataricus lacking CdvB1, these presented a normal constriction of the membrane, but some cells failed to perform the last step of scission, leaving them with two full copies of the genome (Pulschen et al., 2020). Furthermore, cells lacking CdvB2 were able to perform the scission normally, but tended to present a misplacement of the constricting ring, resulting in aberrant daughter cells that were not equally sized (Pulschen et al., 2020). This indicates that the two paralogs responsible for the constriction actually perform different roles during the division process. However, it also shows how cells with any of these two proteins can still perform, albeit with difficulties, the full process of constriction and scission on their own.

While a global picture has thus been emerging, many of the underlying mechanistic interactions remain unclear. CdvA has an E3B domain (ESCRT-III binding region; see Figure 1A) through which it is capable of interacting with the wH (winged helix) region of CdvB (Moriscot et al., 2011). None of the other paralogs present such a wH domain (Caspi et al., 2018). Additionally, CdvA can bind to lipid membranes while CdvB is not able to do so (Samson et al., 2011). Therefore, CdvA is seen as the membrane recruiter of CdvB to the membrane. In turn, CdvB is known to interact with CdvB1, which then interacts with CdvB2 (Samson et al., 2008), suggesting that CdvB is the recruiter of the CdvB1:CdvB2 constricting ring. Finally, during the constriction of the membrane, CdvC is presumed to disassemble the filaments of the CdvB1:CdvB2 polymer to generate a turnover of protein and thus supply energy to the system to deform the membrane (Harker-kirschneck et al., 2022). This ATPase features major structural similarities to the eukaryotic Vps4 (Caillat et al., 2015), which is known to be responsible for the depolymerization of ESCRT-III filaments (Lata et al., 2008; Azad et al., 2023) and to create a turnover of ESCRT-III components at the membrane (Chiaruttini et al., 2015; Pfitzner t al., 2020). In archaea, this similarity is further strengthened by in vitro experiments where CdvC was able to depolymerize CdvB1 filaments and detach CdvB1 from lipid membranes into solution (Blanch Jover et al., 2022).

Little is yet known about how the Cdv proteins are hierarchically recruited to the membrane and how their mutual interactions affect this process. Here, we explore these questions using a bottom-up reconstitution approach. We find that CdvA can bind to lipid membranes, but does so more efficiently when it is interacting with CdvB. We observe that CdvB2 can be recruited to the membrane by both CdvB1 and CdvB. Finally, we show that all Cdv proteins exhibit a preferential binding for highly curved membranes and preferentially localize at the necks of dumbbell-shaped vesicles.

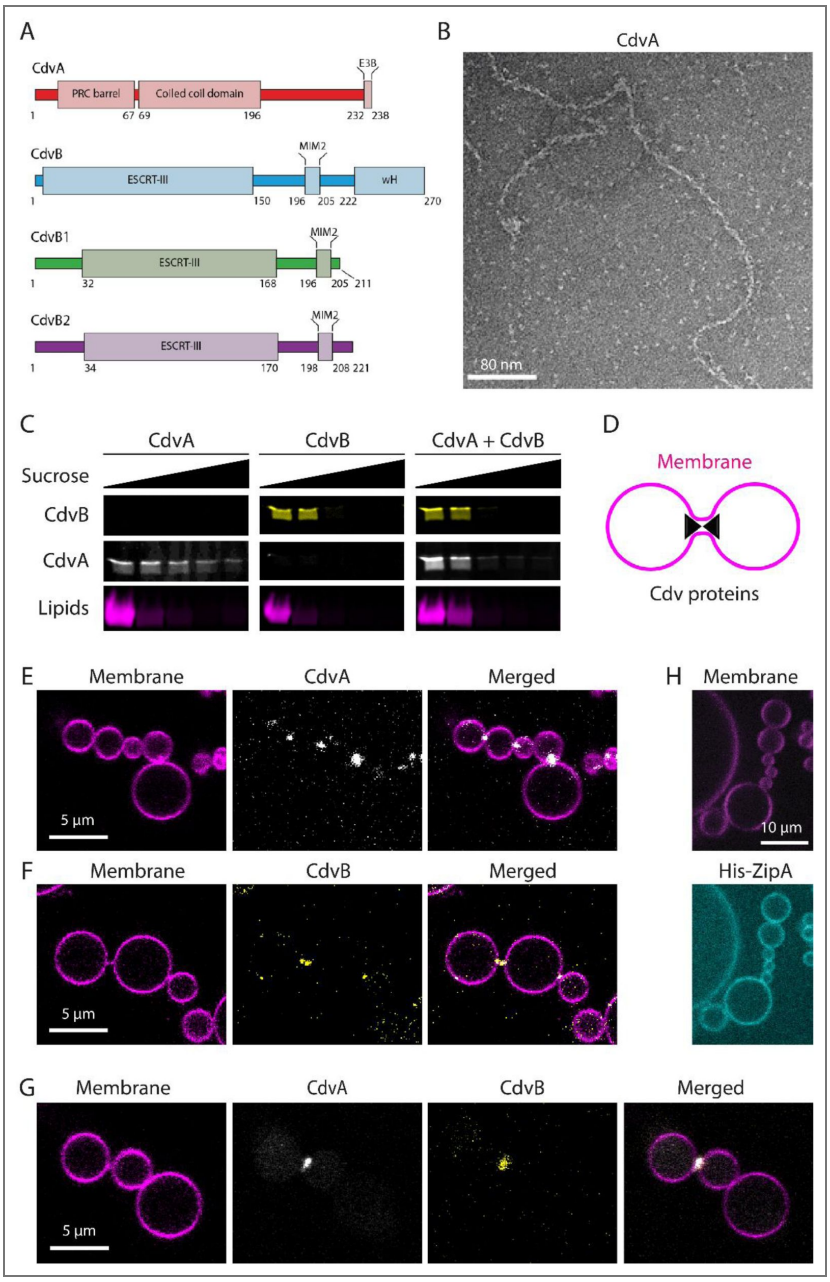

Figure 1. polymerization and membrane binding of CdvA and CdvB

(A) Schematic depicting the domain architecture of Cdv proteins. (B) Negative staining TEM image of elongated filaments formed by CdvA upon removal of the MBP tag in the absence of DNA. (C) Flotation assay showing recombinant Cdv proteins binding to multilamellar vesicles. CdvA alone is distributed in all fractions, while CdvB alone is found predominantly in the liposome-bound fraction. When both CdvA and CdvB are present, both proteins are found predominantly in the liposome-bound fraction. A representative gel from 3 independent experiments is shown. (D) Schematic representing the topology of Cdv proteins reconstituted inside dumbbell-shaped liposomes, recapitulating the shape of a dividing cell. (E) Confocal image of CdvA reconstituted inside dumbbell-shaped liposomes. CdvA localizes at the neck. A representative image from 2 independent experimental preparations is shown. (F) Representative confocal image of CdvB reconstituted inside dumbbell-shaped liposomes. CdvB localizes at the neck. A representative image from 2 independent experimental preparations is shown.(G) Representative confocal image of the CdvA:CdvB complex reconstituted inside dumbbell-shaped liposomes. Both proteins localize at the neck. A representative image from 2 independent experimental preparations is shown. (H) Binding of His-tagged ZipA to dumbbell liposomes containing 18:1 DGS-NTA lipids. As expected for a protein binding the membrane via a His-tag, ZipA exhibits a homogeneous membrane distribution, without enrichment at the neck.

Results

Filament formation by CdvA

Previous in vitro studies of purified CdvA were done with either a full-length version of the protein from M. sedula (Moriscot et al., 2011) or with an N-terminus-truncated CdvA from S. acidocaldarius that was missing the initial PRC barrel (Figure 1A) (Samson et al., 2011; Dobro et al., 2013). The phenotype of these two versions differed in that the full-length protein formed double helical filaments that were reported to be stabilized by the binding of DNA, whereas the N-terminus-truncated CdvA did not polymerize. At the same time, the N-terminus-truncated CdvA was shown to be able to bind to lipid membranes and recruit CdvB to the membrane along with it. For our study, we purified full length CdvA from M. sedula, following the protocol published by Moriscot et al., 2011, and we obtained the same type of filaments as described in their work (Supplementary Figure 1A). However, we never observed interaction between CdvA and lipid membranes (data not shown). We then decided to fuse the full length CdvA to an MBP-tag. The resulting purified MBP-CdvA formed short and thick polymers (Supplementary Figure 1B), which had an average length of 90 ± 40 nm (mean ± SD, N=195) and a width of 12 ± 3 nm (mean ± SD, N=156). When treating the protein with a TEV protease that cleaved the MBP from the protein, CdvA polymerized into long and thin filaments (Figure 1B) with an average length of 220 ± 100 nm (mean ± SD, N=102) and a width of 5 ± 1 nm (mean ± SD, N=106). Formation of these filaments did not require addition of DNA. Thus, the presence of the MBP tag allowed to control the polymerization of CdvA.

CdvB enhances CdvA binding to the membrane

Next, we sought to investigate the lipid-binding capabilities of the full-length CdvA and CdvB. For this, we used a liposome flotation assay, where protein was mixed with negatively charged multilamellar vesicles (see Methods), added to a sucrose gradient, and spun at high speed. This yielded multiple fractions: upper fraction(s) containing liposomes (1), intermediate fraction(s) containing the soluble unbound protein, and the bottom fraction containing protein filaments sedimented at the bottom of the tube. In these assays, we mixed MBP-CdvA with the lipids together with TEV protease, in order to cleave the MBP tag. When testing for the binding of CdvA to lipid membrane, we observed that the protein was distributed to all fractions, including the lipid-bound fraction (Figure 1C). We then purified CdvB which, as previously shown (Moriscot et al., 2011), presented no filamentation regardless of having the MBP-tag or not. In liposome flotation assay, CdvB was highly enriched in the liposome-bound fraction (Figure 1C). In contrast, CdvB from S. acidocaldarius (called Saci_1373) was reported to not show membrane binding on its own (Samson et al., 2011). Thus it appears that CdvB from M. sedula may differ in this regard, although this difference could also be ascribed to different experimental conditions. When CdvA was mixed with CdvB, both proteins were found primarily in the liposome-bound fraction (Figure 1C). This indicates that the binding of full-length CdvA to the lipid membrane is enhanced by CdvB.

The human ESCRT-III system preferentially locates at membrane necks that present high curvatures (De Franceschi et al., 2018; Bertin et al., 2020; Pfitzner et al., 2020). We explored if a similar preference for high curvatures could be observed for Cdv proteins as well. Here, we used a recently developed SMS approach to produce dumbbell-shaped liposomes (De Franceschi et al., 2022). Briefly, a lipid mixture including negatively charged lipids in chloroform was dried out and resuspended in oil. In this oil, we formed water-in-oil droplets in which the proteins were encapsulated, and these droplets were then left to sedimented by gravity through a lipid interface into an outer water phase, thus obtaining unilamellar liposomes that contained the protein on the inside. The outer phase was made of buffer containing DNA “nanostars” that anchor to the membrane, inducing curvature thereby generating dumbbells. We thus obtain chains of dumbbell-shaped liposomes that are mutually connected through membrane necks. Protein that are

encapsulated within these liposomes can be studied for their binding in a membrane geometry that resembles cells that are dividing (Figure 1D). Such a system was recently used to demonstrate a membrane scission activity of Dynamin A (De Franceschi et al., 2024).

In these dumbbell-shaped liposomes, we observed a clear preference of both CdvA, CdvB and the CdvA:CdvB complex to localize at the membrane necks (Figure 1E, 1F, 1G). Proteins displayed a strong fluorescence signal at the membrane necks, while they showed only a residual weak homogeneous binding to other membrane regions of the dumbbell-shaped liposomes. We confirmed that the lobes of these dumbbell-shaped liposomes are connected by membrane necks (Movie 1). We also performed control experiments with a protein that bound the membrane, containing lipids functionalized with Ni-NTA, via a His-tag (ZipA from E. coli) and that was not expected to sense curvature. As expected, ZipA did not show any significant enrichment of the protein signal at the necks (Figure 1H and Supplementary Figure 1C), indicating that the enrichment on highly curved membranes is a specific property of the Cdv proteins and not an artifact induced by the SMS assay.

Filaments formation by CdvB1 and CdvB2ΔC

Next, we purified CdvB2 from M. sedula fused to an MBP-tag. The resulting protein was not presenting any spontaneous filamentation either with or without the MBP tag (Supplementary Figure 2A, 2B). Moreover, we found that full-length CdvB2 was unable to bind membranes in liposome binding assays, neither alone nor in combination with CdvB1 (Supplementary Figure 2C). ESCRT-III proteins commonly feature an inactive soluble state and an active membrane-bound state (Tang et al., 2015). Indeed, *in vitro*, these proteins remain inactive soluble monomers while they may get activated and able to polymerize by deleting their C-terminus part (Shim et al., 2007). The same has been previously shown for purified CdvB (Moriscot et al., 2011), which did not present any polymerization *in vitro*, but spontaneously assembled into filaments upon removal of its C-terminus. Hence, we decided to explore if the same was true for CdvB2, and we made a C-terminal truncated version that contained amino acids 1-170 of CdvB2, henceforth denoted as CdvB2ΔC.

TEM imaging of the CdvB2ΔC-MBP fusion protein showed that it was polymerizing into a characteristic shape of well-defined short linear filaments (Supplementary Figure 2D). Similarly to CdvA, CdvB2ΔC assembled into longer and thinner filaments upon MBP tag cleavage (Figure 2A and Supplementary Figure 2E, 2F), of average length 245 ± 95 nm (mean ± SD; N=36) and width of 14 ± 3 nm (mean ± SD; N=64). These data indicate that CdvB2 also presents a self-inhibitory domain, and that filament formation can be triggered by its removal.

Since CdvB2 forms part of the constricting ring together with CdvB1, we explored the effects of their interaction on filament formation. When mixing CdvB1 and CdvB2ΔC together, filaments formed with a very similar length (272 ± 94 (mean ± SD; N=84)) and width (15 ± 6 (mean ± SD; N=184)) to that of CdvB2ΔC alone (Figure 2B and Supplementary Figure 2E, 2F). Interestingly, these filaments appeared to be more curved. To quantify this, we measured the ratio of the end-to-end distance to the contour length of filaments, which equals 1 for perfectly straight filaments but is <1 for curved ones. For CdvB2ΔC filaments we measured a ratio of 0.86 ± 0.13, while the CdvB1:CdvB2ΔC co-polymer yielded a ratio of 0.75 ± 0.21. This may also imply that the CdvB1:CdvB2ΔC copolymer is more flexible than the CdvB2ΔC homopolymer.

CdvB1 and CdvB2ΔC binding to membrane necks

Subsequently, we tested the ability of CdvB2ΔC to bind lipid membranes. When mixed with negatively charged multilamellar vesicles, CdvB2ΔC was almost exclusively found in the soluble and filamented fractions (Figure 2C), with only a small fraction of the protein found in the lipid-bound fraction. In spite of its low affinity, we encapsulated CdvB2ΔC in dumbbells using the SMS technique and observed instances of CdvB2ΔC clusters at their neck (Figure 2D). It is possible that, in the presence of the correct membrane curvature found at the neck of dumbbells, the affinity of CdvB2ΔC for membrane may increase, indicating that CdvB2ΔC is able to sense curvature. CdvB1 presented clear membrane binding when mixed with liposomes on its own

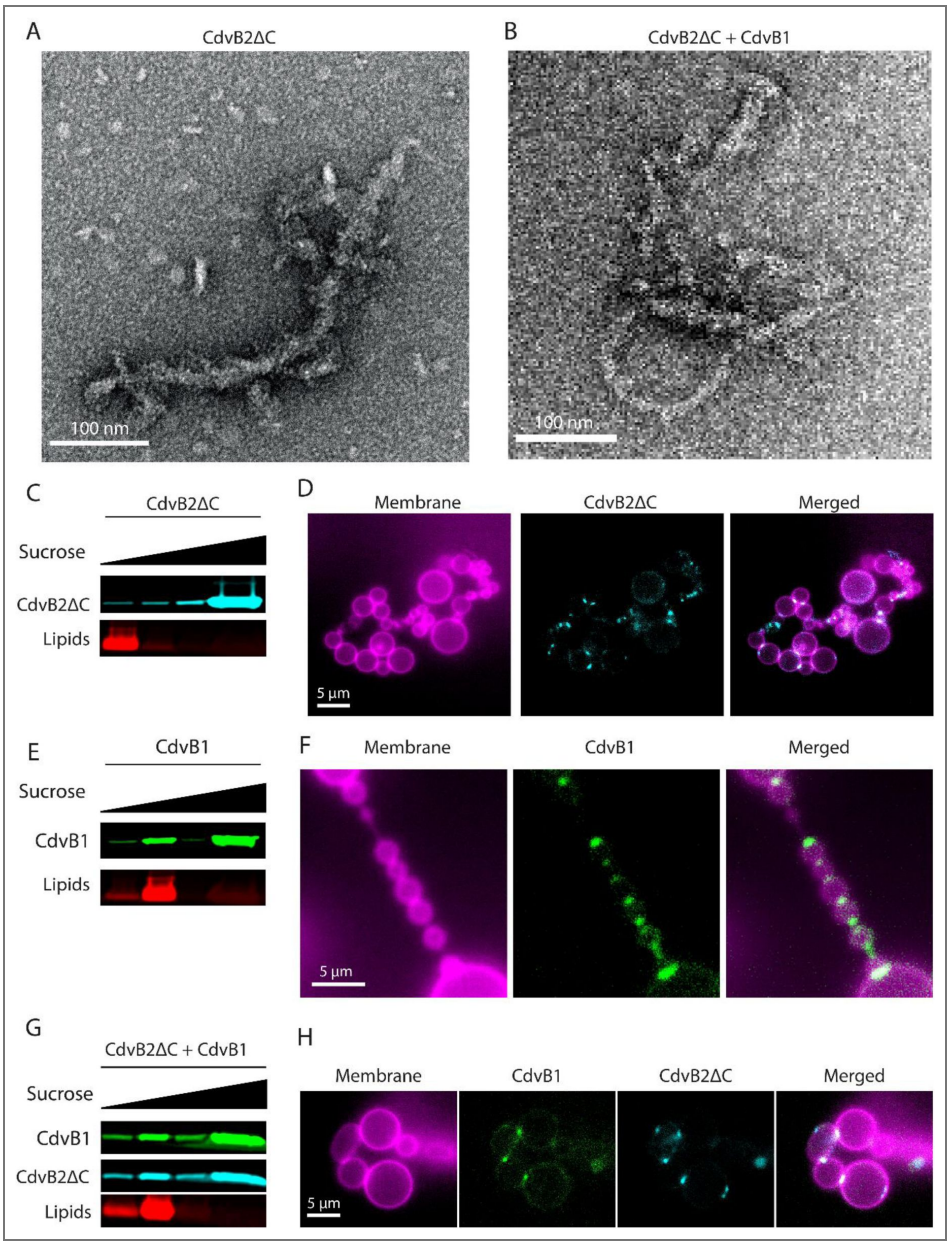

Figure 2. polymerization and membrane binding of the CDVB1: CdvB2ΔC complex.

(A) Negative staining TEM image of CdvB2ΔC filaments obtained upon removal of the MBP tag. (B) Negative staining TEM image of CdvB1:CdvB2ΔC co-polymer. (C) Liposome flotation assays showing very limited membrane binding of CdvB2ΔC alone. A representative gel from 2 independent experimental preparations is shown. (D) Microscopy image of fluorescently labelled CdvB2ΔC reconstituted inside dumbbell-shaped liposomes and localizing at necks. (E) Liposome flotation assays showing clear membrane binding of CdvB1 alone. A representative gel from 2 independent experimental preparations is shown. (F) Microscopy image of fluorescently labelled CdvB1 reconstituted inside dumbbell-shaped liposomes and localizing at necks. (G) Liposome flotation assays showing CdvB2ΔC being recruited to membranes along with CdvB1. A representative gel from 2 independent experimental preparations is shown. (H) Microscopy image of a fluorescently labelled CdvB1:CdvB2ΔC complex reconstituted inside dumbbell-shaped liposomes and localizing at necks.

(Figure 2E), as we previously showed (Blanch Jover et al., 2022). CdvB1 also exhibited preferential neck localization when reconstituted in dumbbells (Figure 2F). When mixing the two proteins and subsequently adding them to multilamellar vesicles, CdvB1 appears to recruit CdvB2ΔC to the membrane (Figure 2G), indicating that they form a complex. Accordingly, we observe binding of the CdvB1:CdvB2ΔC complex to the neck of dumbbell liposomes (Figure 2H).

Reconstitution of a quaternary CdvA:CdvB:CdvB1:CdvB2ΔC complex at a membrane neck

Finally, we explored the interaction between the CdvA:CdvB and CdvB1:CdvB2ΔC complexes in the presence of lipid membranes. In flotation assays, CdvB1 was recruited to the membrane in the presence of CdvA and CdvB (Figure 3A and Supplementary Figure 3A). Moreover, the CdvA:CdvB complex was also able to recruit CdvB2ΔC to liposomes (Figure 3A). Finally, when mixing all four proteins together in the presence of liposomes, we observed that they were all recruited to liposomes (Figure 3A and Supplementary Figure 3B). Thus, our data indicate that either CdvB1 or a CdvA:CdvB complex (or both) can recruit CdvB2 to the membrane.

We then reconstituted the same combinations of Cdv proteins inside dumbbells-shaped liposomes: CdvA (unlabelled) + CdvB + CdvB1 (Figure 3B); CdvA (unlabelled) + CdvB + CdvB2ΔC (Figure 3C) and CdvA (unlabelled) + CdvB + CdvB1 + CdvB2ΔC (Figure 3D). In passing we note that assembly of such a quaternary Cdv complex at membrane necks of dumbbell-shaped liposomes resembling the shape of a dividing cell has never been achieved before. In all cases, we observed a clear preference of the complexes to assemble onto regions of high membrane curvature, as demonstrated by the strong fluorescence signal at the membrane necks. In the quaternary complex, the fluorescence intensity of the Cdv proteins at the necks was about 7 times higher than that at the membrane away from the necks. For comparison, the lipid fluorescence intensity at the neck was only ~2 times enhanced (Supplementary Figure 3C) as expected in the neck region where the membrane of the two lobes are in close proximity.

Discussion

In this study, we elucidated the protein interaction network that governs Cdv protein assembly at the membrane, and showed that Cdv complexes spontaneously localize at membrane necks. We learned that full-length CdvA can form filaments without the need of DNA to stabilize them, and that it binds the membrane to some extent on its own. CdvB from M. sedula binds the membrane efficiently, unlike its homologous from S. acidocaldarius (Samson et al., 2011). When in complex with CdvB, CdvA binds the membrane more efficiently. This suggests that both proteins are likely recruited to the membrane jointly. We confirmed our previous finding that CdvB1 interacts with membranes on its own (Blanch Jover et al., 2022). Furthermore, we purified CdvB2 and showed that it is able to polymerize into filaments once the C-terminal domain is removed. This is a relevant parallelism with the ESCRT machinery, where many of the proteins also only polymerize upon removal of the C-terminus. We observed that CdvB2 binds poorly the membrane by itself, even upon removal of the C-terminal. However, we observed that either CdvB1 or a CdvA:CdvB complex (or both) can recruit CdvB2ΔC to the membrane, which suggests that CdvB2ΔC interaction with the membrane may require these proteins to be present. Intriguingly however, we also observe binding of CdvB2ΔC alone to highly curved membrane, which is the geometry found at the neck of dumbbells. Thus, it is also possible that the mechanism by which CdvB1 and the CdvA:CdvB complex recruit CdvB2ΔC at the membrane is by generating curvature. Further work is needed to thoroughly dissect this phenomenon for the various Cdv proteins.

Recently, in vivo imaging showed that CdvB1 is required to facilitate the spatial separation of CdvB and CdvB2 polymers, as absence of CdvB1 caused a spatial overlapping of CdvB and CdvB2 polymers at the intercellular bridge of dividing cells (Hurtig et al., 2023). Our *in vitro* data show that indeed CdvB2 can be recruited to the membrane by the CdvA:CdvB complex even in the absence of CdvB1. This suggests that the co-localization of CdvB and CdvB2 in the absence of CdvB1 *in vivo* is likely driven by direct interaction between CdvB and CdvB2.

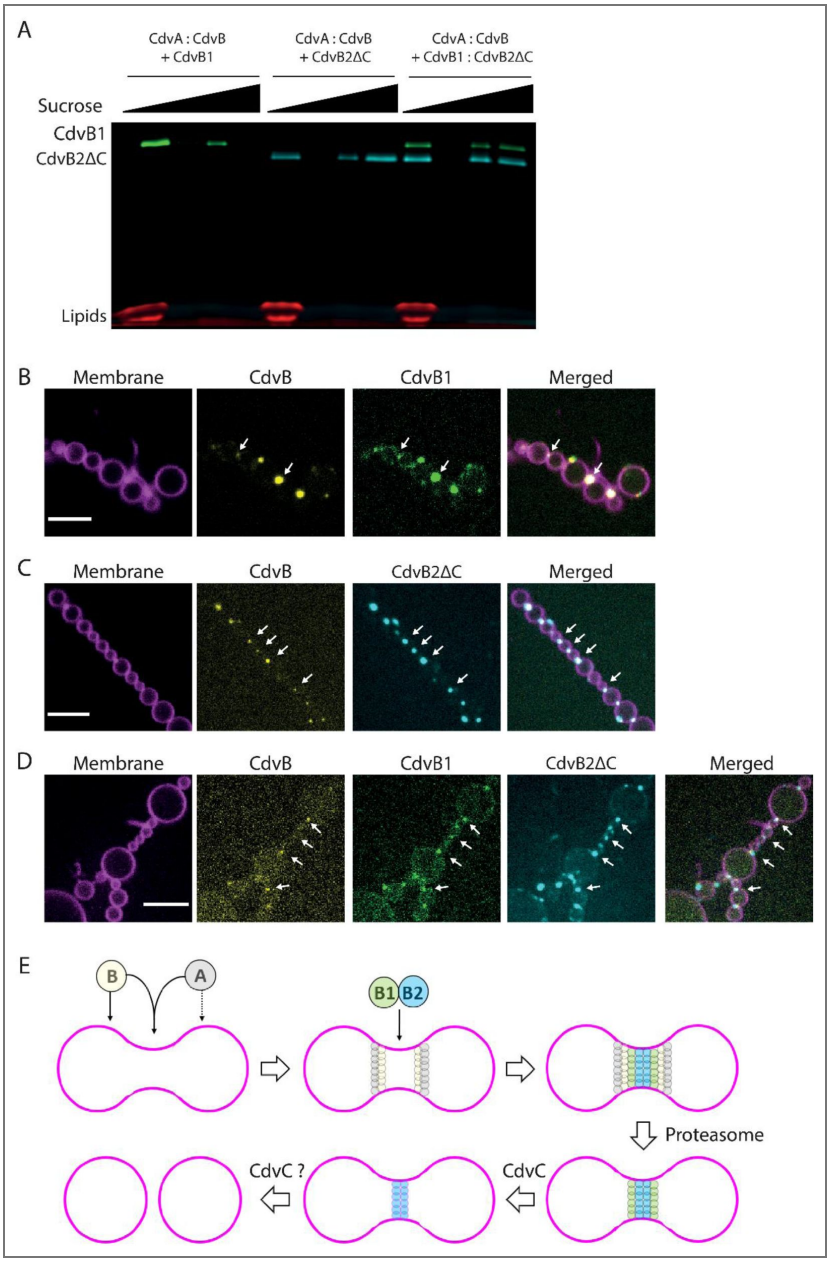

Figure 3. membrane binding of the CdvA:CdvB:CdvB1:CdvB2ΔC quaternary complex

(A) Liposome flotation assays showing recruitment of CdvB1 and CdvB2ΔC to membranes, either alone or in combination, by the CdvA:CdvB complex. (B) Spinning disk confocal images of the ternary complex CdvA (unlabelled) + CdvB-Alexa568 + CdvB1-Alexa488 reconstituted inside the neck of dumbbell liposomes. (C) Spinning disk confocal images of the ternary complex CdvA (unlabelled) + CdvB-Alexa568 + CdvB2ΔC-Cy5 reconstituted inside the neck of dumbbell liposomes. (D) Spinning disk confocal images of the quaternary complex CdvA (unlabelled) + CdvB-Alexa568 + CdvB1-Alexa488 + CdvB2ΔC-Cy5 reconstituted inside the neck of dumbbell liposomes. Scale bars: 10 μm. (E) Schematic depicting the stepwise assembly and disassembly of the Cdv division ring. CdvA and CdvB can bind the membrane individually, but binding of CdvA is enhanced by CdvB, and the two proteins are able to assemble at the neck by forming a complex. Once the CdvA:CdvB ring is assembled, CdvB1 and CdvB2 are both recruited at the neck. Subsequently, the proteasome removes CdvA, and CdvC removes CdvB1, leaving only CdvB2, which may be removed by CdvC, thus achieving membrane abscission.

Moreover, in simulations it was observed that, to obtain a non-overlapping arrangement of Cdv polymers, CdvB1 filaments should be relatively flexible compared to both CdvB and CdvB2 filaments (Hurtig et al., 2023). Our *in vitro* data are consistent with this scenario, as we observe that the CdvB1:CdvB2 co-polymers are more curved, and thus potentially more flexible, than the CdvB2 homo-polymers.

We found that all Cdv proteins preferentially localize at membrane necks, providing the first experimental evidence of affinity of Cdv proteins for high-curvature membranes. This presents another common trait between the archaeal and eukaryotic systems, as many ESCRT proteins also preferentially bind highly curved membranes (Lee et al., 2015; De Franceschi et al., 2018; Bertin et al., 2020; Pfitzner et al., 2020). Notably in our system, we cannot discriminate whether the proteins preferentially assemble on positive or negative curvature, because the neck present in dumbbells exhibits a catenoid geometry, which is characterized by both positive and negative curvature. Using super-resolution microscopy, it was shown that Cdv proteins arrange in ring-like structures that are not completely overlapping; that is, they take distinct spatial positions within the relatively highly curved membrane of the division ring (Hurtig et al., 2023). Our system is currently only amenable for standard confocal microscopy, due to constant moving of the dumbbells (De Franceschi et al., 2022). However, we can envision that protocols for fixation of dumbbells can be developed in the future, which would allow to investigate the assembly of recombinant proteins at the neck region using super-resolution microscopy. This would also help elucidating the nanostructure of CdvA at the neck. Our electron microscopy data show that CdvA assembles in rings that are below the diffraction limit, and accordingly we observe diffraction-limited clusters of CdvA and CdvB at necks. In contract, in vivo CdvA and CdvB were shown to form micrometer-sized rings (Hurtig et al., 2023). One possible interpretation for this discrepancy is that CdvA and CdvB would spontaneously prefer to assemble on a tighter neck, but in vivo they are prevented from doing so by additional factors. This provides a further parallelism with the eukaryotic ESCRT-II complex, in which some subunits may be forced to assemble in vivo in a suboptimal, “frustrated” geometry, and releasing this mechanical frustration could result in membrane deformation (Bertin et al., 2020).

Based on both literature and our own data, we can propose an updated model for the hierarchical assembly of Cdv proteins regulated by protein-protein interactions (Figure 3E): initially, CdvA and CdvB are recruited to the neck via their mutual interaction. Once the CdvA:CdvB complex forms a ring at the membrane, CdvB1 and CdvB2 are also recruited. In our experiment, CdvB1 and CdvB2 can bind the neck even in the absence of a pre-existing CdvA:CdvB complex at the membrane. However, the SMS system itself generates curvature (De Franceschi et al., 2022) and this may favour membrane binding, as our data suggest in the case of CdvB2. *In vivo*, recruitment of CdvB1 and CdvB2 may not occur unless a CdvA:CdvB complex is present. In all our experiments, we observe that CdvB1 and CdvB2ΔC always form a complex, whether in the presence of a membrane or not. Thus is it reasonable to assume that they are also recruited to the CdvA:CdvB complex together. Once the quaternary complex is assembled, CdvB is removed by the proteasome (Tarrason, 2020). In this regard, we provide the crucial piece of evidence that the CdvB1:CdvB2 complex can bind to membrane necks independently of the CdvA:CdvB complex. CdvB1 is subsequently removed from the membrane by CdvC (Blach-Jover, 2022), and here we show that CdvB2 can also bind to membrane necks by itself, without the presence of CdvB1.

We positioned the different subunits in our schematics (Figure 3E) based on their preferred radius of curvature proposed in (Hurtig et al., 2023), obtaining a final arrangement that resembles the later stage of constriction reported in (Hurtig et al., 2023). We expect this arrangement to be the case in our reconstituted system, even though the Cdv proteins are added simultaneously, because the shape of a neck is provided by the SMS system itself (De Franceschi et al., 2022) and therefore each protein can bind to the region having its preferred radius of curvature. This reconstituted system sets the stage to test Cdv-mediated membrane scission in the future, and in particular disassembly of CdvB1 and CdvB2 polymers from membrane necks by the

action of CdvC. This will require the use of a sulfoscope (Pulschen et al., 2020), i.e., a microscope working at elevated temperatures, given that the catalytic activity of CdvC requires high temperature (Blanch Jover et al., 2022).

Methods

Plasmids

All of the proteins that we used are from Metallosphaera sedula., The original plasmids for CdvA (Msed_1670, UniProtID A4YHC3) and CdvB (Msed_1671, UniProtID A4YHC4) were kindly provided to us by Patricia Renesto's lab. From those plasmids, the sequences of the proteins were copied and ordered as a synthetic gene already inserted in a pMAL-c5x from Biomatik, using BamHI and EcoRI cutting sites. Extra codons coding for cysteines were added at the N termini of the proteins for fluorescent labelling. The plasmid for CdvB1 was the same as used in our previous work (8). The gene for CdvB2 (Msed_1695, UniProtID A4YHE8) was obtained from the Gen Bank data base, and was reverse translated using the EMBOSS Backtranseq tool, optimized for E. coli codon usage. To the resulting DNA sequence, a codon of a cysteine for fluorescent labelling was added at the N terminal of the protein, as well as Tobacco Etch Virus (TEV) and an HRV 3C proteases cutting sites. The whole gene construct was ordered as a synthetic gene already inserted in a pMAL-c5x vector from Biomatik, using BamHI and EcoRI cutting sites.

From the original plasmid for MBP-CdvB2, the whole plasmid except for the C-terminus of the protein was copied by PCR. The resulting linearized plasmid was checked on an agarose gel, and then treated with the KLD reaction mix (New England Biolabs, Ipswich, Massachusetts, USA) to digest the template, phosphorylate the ends of the linearized plasmid and ligate it all at once. The reaction mix was then transformed into NEB5alpha competent cells (New England Biolabs), some colonies were picked, and the plasmid was purified using the QIAprep Spin Miniprep Kit (QIAgen, Hilden, Germany) and sent for sequencing.

4.4.2. Protein purification

All proteins were produced in BL-21 E. coli strains. Cells were grown at 37°C in LBamp medium to an OD of around 0.5, at which point expression was induced with IPTG and cells were left to express the protein for 4 hours. After that, cells were harvested by centrifuging at 4500x g at 4°C for 12 minutes. For MBP-CdvA, the cell pellet was resuspended in lysis buffer (50mM Tris pH 8.8, 350 mM NaCl, 50 mM Glutamate, 50 mM Arginine, 0.05mM TCEP, cOmplete™ Protease Inhibitor Cocktail (Roche, Basel, Switzerland)), lysed by French press and centrifuged (150,000 g, 30 min, 4°C). The remaining supernatant was incubated with 1 ml of amylose resin (NEB, Ipswich, Massachusetts, USA) rotating for 2 hours at 4°C, after which it was poured through a gravity chromatography column and the protein was washed (50 mM Tris pH 8.8, 350 mM NaCl, 50 mM Glutamate, 50 mM Arginine, 0.05 mM TCEP) and eluted with elution buffer (50 mM Tris pH 8.8, 350 mM NaCl, 50 mM Glutamate, 50 mM Arginine, 0.05 mM TCEP, 10 mM maltose). For MBP-CdvB, MBP-CdvB2 and MBP-CdvB2ΔC, the cell pellet was resuspended in lysis buffer (50mM Tris pH 8.8, 50 mM NaCl, 0.05 mM TCEP, cOmplete™ Protease Inhibitor Cocktail) lysed by French press and centrifuged (150,000 g, 30 min, 4°C). The remaining supernatant was incubated with 1ml of amylose resin rotating for 2 hours at 4°C, after which it was poured through a gravity chromatography column and the protein was washed (50 mM Tris pH 8.8, 50 mM NaCl, 0.0 5mM TCEP) eluted with elution buffer (50 mM Tris pH 8.8, 50 mM NaCl, 0.05 mM TCEP, 10 mM maltose). MBP-CdvB1 was purified just as described in (8). After affinity chromatography, all proteins were run through a Superdex™ 75 increase 10/300 GL size exclusion chromatography column mounted in an ÄKTA™ Pure system. Samples were run with the same buffer as they were washed and stored by snap freeze in liquid nitrogen. Purity of the samples was evaluated by SDS PAGE stained with Coomassie blue. A fraction of all of the proteins was separated after the affinity chromatography and dialyzed into the same buffer but with pH of 7.4 to perform a maleimide-cysteine conjugation reaction. MBP-CdvA was labelled with Cy5, MBP-CdvB with Alexa-568, MBP-CdvB2ΔC with Cy5 and CdvB1 with Alexa 488. The rest of the purification stayed the same, and excess label was removed from the protein through the gel filtration column.

4.4.3. TEM imaging

For imaging of MBP-CdvA, the protein was diluted down to 100 nM in buffer containing 50 mM Tris pH 7.4 and 50 mM NaCl (all samples were prepared using this buffer). For imaging the protein without MBP, 1μM of MBP-CdvA was mixed with 0.1 μM of TEV protease and left incubating at RT for 1 hour. The sample was then diluted 10 times before depositing it onto a carbon grid. MBP-CdvB2ΔC samples were diluted down to 100 nM in buffer, and samples without MBP were prepared by mixing 1 μM of MBP-CdvB2ΔC with 0.1 μM of TEV protease and left incubating at RT for 1 hour. Samples with CdvB1 and CdvB2ΔC were prepared by mixing MBP-CdvB1 and MBP-CdvB2ΔC both at 1μM concentration with 0.1 μM of TEV protease at RT for 1 hour. The samples were then diluted 10 times before depositing it onto a carbon grid. Samples were absorbed on glow-discharged carbon-coated 400-meshh copper grid purchased from Quantifoil (Großlöbichau, Germany) and stained with 2 % uranyl acetate. They were then imaged on a JEOL JEM-1400plus TEM (JEOL, Akishima, Tokyo, Japan) at 120 kV of accelerating voltage with a TVIPS f416 camera (TVIPS, Gauting, Germany).

4.4.4. Liposome flotation assay

Lipids used were DOPC (1,2-dioleoyl-sn-glycero-3-phosphocholine), DOPG (1,2-dioleoyl-sn-glycero-3-phospho-(1'-rac-glycerol)), and Rhodamine-PE (1,2-dioleoyl-sn-glycero-3-phosphoethanolamine-N-(lissamine rhodamine B sulfonyl)), all of them purchased from Avanti Polar Lipids (Alabaster, Alabama, USA). The lipids, dissolved in chloroform, were mixed to final ratios (mol:mol) of 69.9 DOPC : 30 DOPG : 0.1 Rhodamine-PE, and evaporated in a glass vial to obtain a thin lipid film. Lipids were resuspended in buffer containing 50 mM HEPES pH 7.5, 50 mM NaCl and 300 mM sucrose, at a final concentration of 5 mg/ml. The lipid film was hydrated for 1 hour and thoroughly vortexed to form multilamellar vesicles. The lipids were then mixed with 0.1 μM of TEV protease and 1 μM of protein of interest. Lipids and protein were left to incubate for 1 hour at RT. The sample was then deposited at the bottom of an ultracentrifuge tube, and mixed with buffer containing sucrose to obtain a bottom layer of 30% of sucrose. Gently, another layer of buffer with 25% of sucrose was deposited, and a final layer of 0% of sucrose on top. In the experiments shown in Figure 1C, the sample was instead applied to the top of the sucrose gradient. Then it was centrifuged at 200,000 g at 4 °C for 30 minutes in a SW 60 Ti Swinging Bucket rotor. All the different fractions of the sucrose gradient were then pipetted out and extra buffer was then added to resuspend the filamented pellet at the bottom. The different fractions were then analysed by SDS PAGE, and the presence of the proteins was visualize either by the fluorescence of the fluorophore-labelled proteins or by staining with Coomassie blue. Experiments with CdvB2ΔC were done with a final concentration of all the proteins of 600nM, and gels were imaged using a GE Amersham™ Typhoon gel imager to image the fluorescent label on the proteins and lipids.

4.4.5. Preparation of lipid in oil suspension for dumbbell-shaped liposome preparations

DOPC, DOPE-PEG2000, DOPG and DOPE-Rhodamine (or DOPE-Atto390 for experiments with proteins with overlapping fluorescence) in chloroform were mixed in a ratio of 93:2:5:0.1 and evaporated in a glass vial under a blow of nitrogen. Lipid mixture was then resolubilized in chloroform to a final concentration of 0.2 mg/ml. A freshly prepared mixture of silicone and mineral oil that was added to the lipids in chloroform slowly dropwise while vortexing gently. After all oil is added to the chloroform, it was vortexed at max speed for 2 minutes and then sonicated for 15 minutes in an ice bath.

4.4.6. Preparation of dumbbell-shaped liposomes with the synthetic membrane shaper

Cdv proteins were mixed in an inner buffer containing 50mM Tris pH 7.5 and 37 % w/v optiprep (Sigma Aldrich, St. Louis, Missouri, USA) to make the solution heavy. In parallel, an outer solution in buffer containing 50 mM Tris pH7.4, 5 mM MgCl2 and glucose to match the osmolarity of the outer solution at 30 mOsm higher than in the inner solution. The DNA nanostars developed in Ref. (24) were then mixed into the outer solution and deposited at the bottom of an imaging chamber.

Water in oil droplets of inner buffer containing protein were then formed by pipetting up and down 20 µl of inner solution into 400 µl of oil until a homogeneous droplet size was achieved. The droplets in oil were immediately deposited on top of the outer solution in the imaging chamber, and they were allowed to sediment by gravity through the oil-water interphase. The liposomes were imaged using spinning disk confocal laser microscopy (Olympus IXB1/BX61 microscope, 60× objective, iXon camera) with Andor iQ3 software. Analysis of the images was done with ImageJ (v.2.1.0).

Data availability

All data associated with this article are available upon request to the corresponding author: Cees Dekker C.Dekker@tudelft.nl

Acknowledgements

We thank Eli van der Sluis and Ashmiani van den Berg for discussions and protein purification. We acknowledge funding support from the BaSyC program of NWO-OCW and from the ERC Advanced Grant 883684. This research is part of the project no. 2022/45/P/NZ1/01565 co-funded by the National Science Centre and the European Union Framework Programme for Research and Innovation Horizon 2020 under the Marie Skłodowska-Curie grant agreement no. 945339.

Additional files

Supplementary Figures 1, 2, and 3.

Additional information

Funding

Funder	Grant reference number	Author
EC | European Research Council (ERC)	https://doi.org/10.3030/883684	Alberto Blanch-Jover Cees Dekker
National Science Centre Poland	2022/45/P/NZ1/01565	Nicola De Franceschi
NWO-OCW	BaSyC program	Nicola De Franceschi Alberto Blanch-Jover
EC | Horizon 2020 Framework Programme (H2020)	https://doi.org/10.3030/945339	Nicola De Franceschi

Author ORCID iDs

Nicola De Franceschi: https://orcid.org/0000-0002-7221-613X
Alberto Blanch-Jover: https://orcid.org/0000-0002-1484-7793
Cees Dekker: https://orcid.org/0000-0001-6273-071X

References

Azad K, Guilligay D, Boscheron C, Maity S, De Franceschi N, Sulbaran G, Effantin G, Wang H, Kleman JP, Bassereau P, *et al.* (2023) Structural basis of CHMP2A-CHMP3 ESCRT-III polymer assembly and membrane cleavage. *Nat Struct Mol Biol* **30**:81-90

Bertin A, de Franceschi N, de la Mora E, Maity S, Alqabandi M, Miguet N, di Cicco A, Roos WH, Mangenot S, Weissenhorn W, *et al.* (2020) Human ESCRT-III polymers assemble on positively curved membranes and induce helical membrane tube formation. *Nat Commun* **11**:2663

Blanch Jover A, De Franceschi N, Fenel D, Weissenhorn W, Dekker C (2022) The archaeal division protein CdvB1 assembles into polymers that are depolymerized by CdvC. *FEBS Lett* **596**:958-969

Caillat C, Macheboeuf P, Wu Y, McCarthy AA, Boeri-Erba E, Effantin G, Göttlinger HG, Weissenhorn W, Renesto P (2015) Asymmetric ring structure of Vps4 required for ESCRT-III disassembly. *Nat Commun* **6**:8781

Caspi Y, Dekker C (2018) Dividing the Archaeal Way: The Ancient Cdv Cell-Division Machinery. *Front Microbiol* **9**:174

Chiaruttini N, Redondo-Morata L, Colom A, Humbert F, Lenz M, Scheuring S, Roux A (2015) Relaxation of Loaded ESCRT-III Spiral Springs Drives Membrane Deformation. *Cell* **163**:866-79

Cox CJ, Foster PG, Hirt RP, Harris SR, Embley TM (2008) The archaebacterial origin of eukaryotes. *Proc Natl Acad Sci U S A* **105**:20356-61

De Franceschi N, Alqabandi M, Miguet N, Caillat C, Mangenot S, Weissenhorn W, Bassereau P (2018) The ESCRT protein CHMP2B acts as a diffusion barrier on reconstituted membrane necks. *J Cell Sci* **132**:jcs217968

De Franceschi N, Barth R, Meindlhumer S, Fragasso A, Dekker C (2024) Dynamin A as a one-component division machinery for synthetic cells. *Nat Nanotechnol* **19**:70-76

De Franceschi N, Pezeshkian W, Fragasso A, Bruininks BMH, Tsai S, Marrink SJ, Dekker C (2022) Synthetic Membrane Shaper for Controlled Liposome Deformation. *ACS Nano* **17**:966-78

Dobro MJ, Samson RY, Yu Z, McCullough J, Ding HJ, Chong PL, Bell SD, Jensen GJ (2013) Electron cryotomography of ESCRT assemblies and dividing Sulfolobus cells suggests that spiraling filaments are involved in membrane scission. *Mol Biol Cell* **24**:2319-27

Harker-Kirschneck L, Hafner AE, Yao T, Vanhille-Campos C, Jiang X, Pulschen A, Hurtig F, Hryniuk D, Culley S, Henriques R, *et al.* (2022) Physical mechanisms of ESCRT-III-driven cell division. *Proc Natl Acad Sci U S A* **119**:e2107763119

Hurley JH (2015) ESCRTs are everywhere. *EMBO J* **34**:2398-407

Hurtig F, Burgers TCQ, Cezanne A, Jiang X, Mol FN, Traparić J, Pulschen AA, Nierhaus T, Tarrason-Risa G, Harker-Kirschneck L, *et al.* (2023) The patterned assembly and stepwise Vps4-mediated disassembly of composite ESCRT-III polymers drives archaeal cell division. *Sci Adv* **9**:eade5224

Lata S, Schoehn G, Jain A, Pires R, Piehler J, Gottlinger HG, Weissenhorn W (2008) Helical structures of ESCRT-III are disassembled by VPS4. *Science* **321**:1354-7

Lee IH, Kai H, Carlson LA, Groves JT, Hurley JH (2015) Negative membrane curvature catalyzes nucleation of endosomal sorting complex required for transport (ESCRT)-III assembly. *Proc Natl Acad Sci U S A* **112**:15892-7

Lindås AC, Karlsson EA, Lindgren MT, Ettema TJ, Bernander R (2008) A unique cell division machinery in the Archaea. *Proc Natl Acad Sci U S A* **105**:18942-6

Makarova KS, Yutin N, Bell SD, Koonin EV (2010) Evolution of diverse cell division and vesicle formation systems in Archaea. *Nat Rev Microbiol* **8**:731-41

Moriscot C, Gribaldo S, Jault JM, Krupovic M, Arnaud J, Jamin M, Schoehn G, Forterre P, Weissenhorn W, Renesto P (2011) Crenarchaeal CdvA forms double-helical filaments containing DNA and interacts with ESCRT-III-like CdvB. *PLoS One* **6**:e21921

Pfitzner AK, Mercier V, Jiang X, von Filseck J Moser, Baum B, Šarić A, Roux A (2020) An ESCRT-III Polymerization Sequence Drives Membrane Deformation and Fission. *Cell* **182**:1140-1155.

Pulschen AA, Mutavchiev DR, Culley S, Sebastian KN, Roubinet J, Roubinet M, Risa GT, van Wolferen M, Roubinet C, Schmidt U, *et al.* (2020) Live Imaging of a Hyperthermophilic Archaeon Reveals Distinct Roles for Two ESCRT-III Homologs in Ensuring a Robust and Symmetric Division. *Curr Biol* **30**:2852-2859.

Samson RY, Obita T, Freund SM, Williams RL, Bell SD (2008) A role for the ESCRT system in cell division in archaea. *Science* **322**:1710-3

Samson RY, Obita T, Hodgson B, Shaw MK, Chong PL, Williams RL, Bell SD (2011) Molecular and structural basis of ESCRT-III recruitment to membranes during archaeal cell division. *Mol Cell* **41**:186-96

Shim S, Kimpler LA, Hanson PI (2007) Structure/function analysis of four core ESCRT-III proteins reveals common regulatory role for extreme C-terminal domain. *Traffic* **8**:1068-79

Schöneberg J, Lee IH, Iwasa JH, Hurley JH (2017) Reverse-topology membrane scission by the ESCRT proteins. *Nat Rev Mol Cell Biol* **18**:5-17

Tang S, Henne WM, Borbat PP, Buchkovich NJ, Freed JH, Mao Y, Fromme JC, Emr SD (2015) Structural basis for activation, assembly and membrane binding of ESCRT-III Snf7 filaments. *eLife* **4**:e12548 https://doi.org/10.7554/eLife.12548

Tarrason Risa G, Hurtig F, Bray S, Hafner AE, Harker-Kirschneck L, Faull P, Davis C, Papatziamou D, Mutavchiev DR, Fan C, *et al.* (2020) The proteasome controls ESCRT-III-mediated cell division in an archaeon. *Science* **369**:eaaz2532

Peer reviews

Reviewer #1 (Public review):

Summary:

The authors aimed to elucidate the recruitment order and assembly of the Cdv proteins during Sulfolobus acidocaldarius archaeal cell division using a bottom-up reconstitution approach. They employed liposome-binding assays, EM, and fluorescence microscopy with in vitro reconstitution in dumbbell-shaped liposomes to explore how CdvA, CdvB, and the homologues of ESCRT-III proteins (CdvB, CdvB1, and CdvB2) interact to form membrane remodeling complexes.

The study sought to reconstitute the Cdv machinery by first analyzing their assembly as two sub-complexes: CdvA:CdvB and CdvB1:CdvB2ΔC. The authors report that CdvA binds lipid membranes only in the presence of CdvB and localizes preferentially to membrane necks. Similarly, the findings on CdvB1:CdvB2ΔC indicate that truncation of CdvB2 facilitates filament formation and enhances curvature sensitivity in interaction with CdvB1. Finally, the authors reconstitute a quaternary CdvA:CdvB:CdvB1:CdvB2 complex and demonstrate its enrichment at membrane necks. The mechanistic details of how these complexes drive membrane remodeling, particularly through subcomplex removal by the proteasome and/or CdvC, remain insufficiently addressed, and the study therefore mainly provides an experimental framework for future mechanistic investigation.

Strengths:

The study of machinery assembly and its involvement in membrane remodeling, particularly using bottom-up reconstituted in vitro systems, presents significant challenges. This is particularly true for systems like the ESCRT-III complex, which localizes uniquely at the lumen of membrane necks prior to scission. The use of dumbbell-shaped liposomes in this study provides a promising experimental model to investigate ESCRT-III and ESCRT-III-like protein activity at membrane necks.

The authors present intriguing evidence regarding the sequential recruitment of ESCRT-III proteins in crenarchaea-a close relative of eukaryotes.

Weaknesses:

The findings of this study suggest that the hierarchical recruitment characteristic of eukaryotic systems may predate eukaryogenesis, which represents a significant and exciting contribution. However, the broader implications of these findings for membrane remodeling mechanisms remain largely unexplored. Nevertheless, this study provides a valuable experimental framework to address these questions in the future.

https://doi.org/10.7554/eLife.104226.2.sa3

Reviewer #2 (Public review):

Summary:

The Crenarchaeal Cdv division system represents a reduced form of the universal and ubiquitous ESCRT membrane reverse-topology scission machinery, and therefore a prime candidate for synthetic and reconstitution studies. The work here represents a convincing extension of previous work in the field, clarifying the order of recruitment of Cdv proteins to curved membranes.

Strengths:

The use of a recently developed approach to produce dumbbell-shaped liposomes (De Franceschi et al. 2022), which allowed the authors to assess recruitment of various Cdv assemblies to curved membranes or membrane necks; reconstitution of a quaternary Cdv complex at a membrane neck.

Weaknesses:

The initial manuscript was a bit light on quantitative detail, across the various figures - addressing this would make the paper much stronger. The authors could also include in the discussion a short paragraph on implications for our understanding of ESCRT function in other contexts and/or in archaeal evolution - for the interests of a broad audience. These issues have been addressed in the authors' revision.

https://doi.org/10.7554/eLife.104226.2.sa2

Reviewer #3 (Public review):

In this revised report, De Franceschi et al. purify components of the Cdv machinery in archaeon M. sedula and probe their interactions with membrane and with one-another in vitro using two main assays - liposome flotation and fluorescent imaging of encapsulated proteins. This has the potential to add to the field by showing how the order of protein recruitment seen in cells is related to the differential capacity of individual proteins to bind membranes when alone or when combined.

Using the floatation assay, they demonstrate that CdvA, CdvB, and CdvB1 bind liposomes. CdvB2 lacking its C-terminus is not efficiently recruited to membranes unless CdvAB or CdvB1 are present. The authors then employ a clever liposome assay that generates chained spherical liposomes connected by thin membrane necks, which allows them to accurately control the buffer composition inside and outside of the liposome. With this, they show that all four proteins accumulate in necks of dumbbell-shaped liposomes that mimic the shape of constricting necks in cell division, possibly indicating a sensing of catenoid membrane

geometry. Taken altogether, these data lead them to propose that Cdv proteins are sequentially recruited to the membrane as has also been suggested by in vivo studies of ESCRT-III dependent cell division in crenarchaea.

In their revision, the authors have addressed the vast majority of our previous concerns. The paper is much improved as a result. The Figures are improved and the authors have added appropriate controls and additional experiments, strengthening their conclusions.

There are still some discrepancies between these results and what is know about Sulfolobus division. Since the initial submission, other work has shown that in S. acidocaldarius, CdvA is the first component to assemble a ring (in absence of CdvB , doi.org/10.1073/pnas.2513939122) and that CdvB2 is able to bind membranes in vitro (doi.org/10.1073/pnas.2525941123). This might reflect differences between Sulfolobus and Metallosphaera, but probably should be discussed.

https://doi.org/10.7554/eLife.104226.2.sa1

Author response:

The following is the authors' response to the original reviews

Public Reviews:

Reviewer #1 (Public review):

Summary:

The authors aimed to elucidate the recruitment order and assembly of the Cdv proteins during Sulfolobus acidocaldarius archaeal cell division using a bottom-up reconstitution approach. They employed liposome-binding assays, EM, and fluorescence microscopy with in vitro reconstitution in dumbbellshaped liposomes to explore how CdvA, CdvB, and the homologues of ESCRT-III proteins (CdvB, CdvB1, and CdvB2) interact to form membrane remodeling complexes.

The study sought to reconstitute the Cdv machinery by first analyzing their assembly as two subcomplexes: CdvA:CdvB and CdvB1:CdvB2ΔC. The authors report that CdvA binds lipid membranes only in the presence of CdvB and localizes preferentially to membrane necks. Similarly, the findings on CdvB1:CdvB2ΔC indicate that truncation of CdvB2 facilitates filament formation and enhances curvature sensitivity in interaction with CdvB1. Finally, while the authors reconstitute a quaternary CdvA:CdvB:CdvB1:CdvB2 complex and demonstrate its enrichment at membrane necks, the mechanistic details of how these complexes drive membrane remodeling by subcomplexes removal by the proteasome and/or CdvC remain speculative.

Although the work highlights intriguing similarities with eukaryotic ESCRT-III systems and explores unique archaeal adaptations, the conclusions drawn would benefit from stronger experimental validation and a more comprehensive mechanistic framework.

Strengths:

The study of machinery assembly and its involvement in membrane remodeling, particularly using bottom-up reconstituted in vitro systems, presents significant challenges. This is particularly true for systems like the ESCRT-III complex, which localizes uniquely at the lumen of membrane necks prior to scission. The use of dumbbell-shaped liposomes in this study provides a promising experimental model to investigate ESCRT-III and ESCRT-III-like protein activity at membrane necks.

> *The authors present intriguing evidence regarding the sequential recruitment of ESCRT-III proteins in crenarchaea-a close relative of eukaryotes. This finding suggests that the hierarchical recruitment characteristic of eukaryotic systems may predate eukaryogenesis, which is a significant and exciting contribution. However, the broader implications of these findings for membrane remodeling mechanisms remain speculative, and the study would benefit from stronger experimental validation and expanded contextualization within the field.*

We thank the Referee for his/her appreciation of our work.

> *Weaknesses:*
>
> *This manuscript presents several methodological inconsistencies and lacks key controls to validate its claims. Additionally, there is insufficient information about the number of experimental repetitions, statistical analyses, and a broader discussion of the major findings in the context of open questions in the field.*

We have now added more controls, information about repetitions, and discussion.

> ***Reviewer #2 (Public review):***
>
> *Summary:*
>
> *The Crenarchaeal Cdv division system represents a reduced form of the universal and ubiquitous ESCRT membrane reverse-topology scission machinery, and therefore a prime candidate for synthetic and reconstitution studies. The work here represents a solid extension of previous work in the field, clarifying the order of recruitment of Cdv proteins to curved membranes.*
>
> *Strengths:*
>
> *The use of a recently developed approach to produce dumbbell-shaped liposomes (De Franceschi et al. 2022), which allowed the authors to assess recruitment of various Cdv assemblies to curved membranes or membrane necks; reconstitution of a quaternary Cdv complex at a membrane neck.*

We thank the Referee for his/her appreciation of the work.

> *Weaknesses:*
>
> *The manuscript is a bit light on quantitative detail, across the various figures, and several key controls are missing (CdvA, B alone to better interpret the co-polymerisation phenotypes and establish the true order of recruitment, for example) - addressing this would make the paper much stronger. The authors could also include in the discussion a short paragraph on implications for our understanding of ESCRT function in other contexts and/or in archaeal evolution, as well as a brief exploration of the possible reasons for the discrepancy between the foci observed in their liposome assays and the large rings observed in cells - to better serve the interests of a broad audience.*

We have now added more controls, information about repetitions, and discussion.

> ***Reviewer #3 (Public review):***
>
> *Summary:*
>
> *In this report, De Franceschi et al. purify components of the Cdv machinery in archaeon M. sedula and probe their interactions with membrane and with one-another in vitro using two main assays - liposome flotation and fluorescent imaging of encapsulated*

> *proteins. This has the potential to add to the field by showing how the order of protein recruitment seen in cells is related to the differential capacity of individual proteins to bind membranes when alone or when combined.*
>
> *Strengths:*
>
> *Using the floatation assay, they demonstrate that CdvA and CdvB bind liposomes when combined. While CdvB1 also binds liposomes under these conditions, in the floatation assay, CdvB2 lacking its C-terminus is not efficiently recruited to membranes unless CdvAB or CdvB1 are present. The authors then employ a clever liposome assay that generates chained spherical liposomes connected by thin membrane necks, which allows them to accurately control the buffer composition inside and outside of the liposome. With this, they show that all four proteins accumulate in necks of dumbbell-shaped liposomes that mimic the shape of constricting necks in cell division. Taken altogether, these data lead them to propose that Cdv proteins are sequentially recruited to the membrane as has also been suggested by in vivo studies of ESCRT-III dependent cell division in crenarchaea.*

We thank the Referee for his/her appreciation of the work.

> *Weaknesses:*
>
> *These experiments provide a good starting point for the in vitro study the interaction of Cdv system components with the membrane and their consecutive recruitment. However, several experimental controls are missing that complicate their ability to draw strong conclusions. Moreover, some results are inconsistent across the two main assays which make the findings difficult to interpret:*
>
> *(1) Missing controls.*
>
> *Various protein mixtures are assessed for their membrane-binding properties in different ways. However, it is difficult to interpret the effect of any specific protein combination, when the same experiment is not presented in a way that includes separate tests for all individual components. In this sense, the paper lacks important controls. For example, Fig 1C is missing the CdvB-only control. The authors remark that CdvB did not polymerise (data not shown) but do not comment on whether it binds membrane in their assays. In the introduction, Samson et al., 2011 is cited as a reference to show that CdvB does not bind membrane. However, here the authors are working with protein from a different organism in a different buffer, using a different membrane composition and a different assay. Given that so many variables are changing, it would be good to present how M. sedula CdvB behaves under these conditions.*

We thank the referee for raising this point. We have now added these data in Figure 1C. Indeed it turns out that CdvB from *M. sedula* exhibits clear membrane binding on its own in a flotation assay.

> *Similarly, there is no data showing how CdvB alone or CdvA alone behave in the dumbbell liposome assay.*

Without these controls, it's impossible to say whether CdvA recruits CdvB or the other way around. The manuscript would be much stronger if such data could be added.

We have now added these data in Figure 1E, 1F and 1G. Overall, we can confirm that CdvA binds the membrane better in the presence of CdvB (although both proteins can bind the membrane on their own). Both proteins appear to recognize the curved region of the membrane neck.

> *(2) Some of the discrepancies in the data generated using different assays are not discussed.*
>
> *The authors show that CdvB2ΔC binds membrane and localizes to membrane necks in the dumbbell liposome assay, but no membrane binding is detected in the flotation assay. The discrepancy between these results further highlights the need for CdvB-only and CdvA-only controls.*

We have now added these controls in Figure 1. In addition, we would like to clarify that the flotation assay and the SMS dumbbell assay serve different purposes and are not directly comparable in quantitative terms. In the flotation assay, all the protein present as input is eventually recovered and visualized. Thus, quantitative information on the proportion of the fraction of the total protein bound to lipids can be inferred from this assay. The SMS assay, in contrast, provides a very different kind of information. Because of the particular protocol required to generate dumbbells (De Franceschi, 2022), the total amount of protein in the inner buffer in dumbbells is not accurately defined, because protein that is not correctly reconstituted (e.g. which aggregates while still in the droplet phase) will interfere with vesicle generation, with the result that dumbbell with such aggregates is generally not formed in the first place. This renders it impossible to draw any quantitative conclusions about the proportion of the sample bound to lipids. The SMS is therefore not directly comparable to the flotation assay, and it is rather complementary to it. Indeed, the purpose of the SMS is to provide information about curvature selectivity of the protein.

> *(3) Validation of the liposome assay.*
>
> *The experimental setup to create dumbbell-shaped liposomes seems great and is a clever novel approach pioneered by the team. Not only can the authors manipulate liposome shape, they also state that this allows them to accurately control the species present on the inside and outside of the liposome. Interpreting the results of the liposome assay, however, depends on the geometry being correct. To make this clearer, it would seem important to include controls to prove that all the protein imaged at membrane necks lie on the inside of liposomes. In the images in SFig3 there appears to be protein outside of the liposome. It would also be helpful to present data to show test whether the necks are open, as suggested in the paper, by using FRAP or some other related technique.*

We thank the Referee for his/her appreciation. The proteins are encapsulated inside the liposomes, not outside of them. While Figure S3 might give the appearance that there is some protein outside, this is actually just an imaging artifact. Author response image 1 (below) explains this: When the membrane and protein channel are shown separately, it is clear that the protein cluster that appeared to be 'outside' actually colocalizes with an extra small dumbbell lobe (yellow arrowhead). The protein appeared to be outside of it because (1) the protein fluorescent signal is stronger than the signal from the membrane, and (2) there is a certain time delay in the acquisition of the two channels (0.5-1 second), thus the membrane may have slightly shifted out of focus when the fluorescence was being acquired. We are confident that the protein is inside in these dumbbells because the procedure for preparing the dumbbells requires extensive emulsification by pipetting, which requires ≈ 1 minute. This time is more than sufficient for proteins with high affinity for the membrane, like ESCRT and Cdv, to bind the membrane. For an example of how fast binding under confinement can be, please see movie 2 from this paper: De Franceschi N, Alqabandi M, Miguet N, Caillat C, Mangenot S, Weissenhorn W, Bassereau P. The ESCRT protein CHMP2B acts as a diffusion barrier on reconstituted membrane necks. J Cell Sci. 2018 Aug 3;132(4):jcs217968.

Moreover, in many instances, we observed that the protein is inside because, by increasing the gain in the images post-acquisition, a clear protein signal appear in the lumen (see Author response image 2).

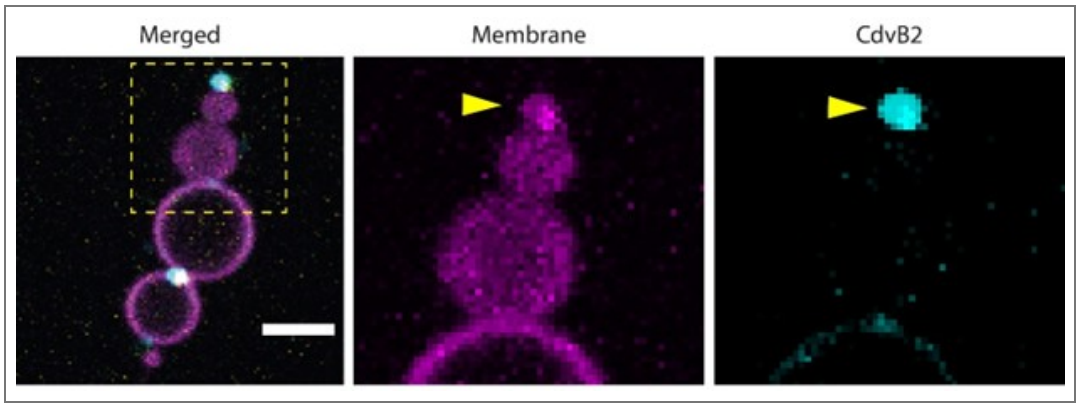

Author response image 1. Separate channels showing colocalization of protein and lipids (adapted from Figure S3). The zoom-in shows separate channels, highlighting that the CdvB2 cluster that seems to be 'outside the dumbbell' actually colocalizes with the small terminal lobe of the dumbbell, indicating that the protein is encapsulated within that lobe.

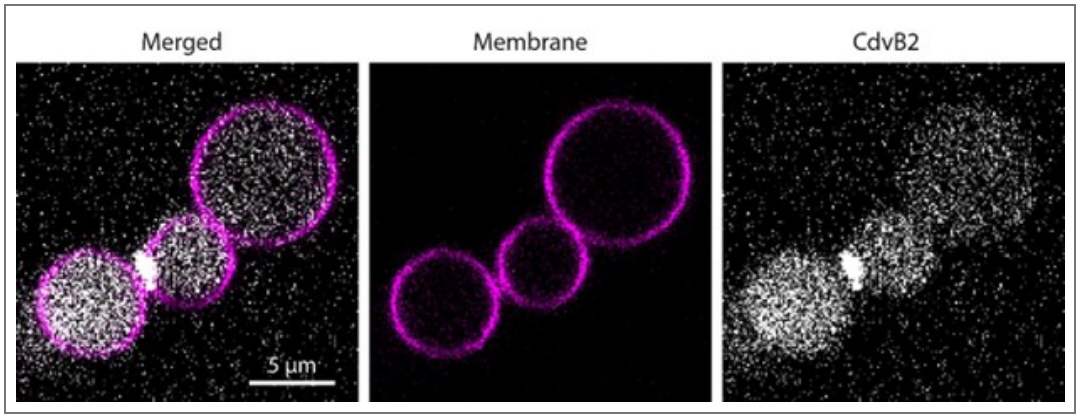

Author response image 2. Residual protein present inside lumen of dumbbells as visualized by increasing the brightness post-acquisition.

We are not sure what the referee means by "test whether the necks are open, as suggested in the paper". We are confident that the lobes of dumbbells originated from a single floppy vesicle, and were therefore mutually connected with an open neck (at least at the onset of the experiment). We have performed extensive FRAP assays on dumbbells in previous papers (De Franceschi et al., ACS nano 2022 and De Franceschi et al., Nature Nanotech 2024) which unequivocally proved that these chains of dumbbells are connected with open necks. We now also performed a few FRAP assay with reconstituted Cdv proteins, which confirmed this point. We have added a movie of such an experiment to the manuscript (Movie 1).

Investigating whether the necks are open or closed after Cdv reconstitution is indeed a very relevant question, that could be rephrased as "verify whether Cdv proteins or their combination can induce membrane scission". This is however beyond the scope of this manuscript, as the current work merely addressed the question of hierarchical recruitment of Cdv proteins at the membrane. We plan to examine this in future work.

> *(4) Quantification of results from the liposome assay.*
>
> *The paper would be strengthened by the inclusion of more quantitative data relating to the liposome assay. Firstly, only a single field of view is shown for each condition. Because of this, the reader cannot know whether this is a representative image, or an outlier? Can the authors do some quantification of the data to demonstrate this? The line*

> *scan profiles in the supplemental figures would be an example of this, but again in these Figures only a single image is analyzed.*

The images that we showed are indeed representative. The dumbbells that are generated by the SMS approach contain an "internal control": in each dumbbell, the protein has the option of localizing at the neck or localizing elsewhere in the region of flat membrane. We see consistently that Cdv proteins have a strong preference for localizing at the neck.

> *We would recommend that the authors present quantitative data to show the extent of co-localization at the necks in each case. They also need a metric to report instances in which protein is not seen at the neck, e.g. CdvB2 but not CdvB1 in Fig2I, which rules out a simple curvature preference for CdvB2 as stated in line 182.*

While the request for better quantitation is reasonable, this would require carrying out very significant new experiments at the microscope, which is rendered near-impossible since both first authors left the lab on to new positions.

> *Secondly, the authors state that they see CdvB2ΔC recruited to the membrane by CdvB1 (lines 184-187, Fig 2I). However, this simple conclusion is not borne out in the data. Inspecting the CdvB2ΔC panels of Fig 2I, Fig3C, and Fig3D, CdvB2ΔC signal can be seen at positions which don't colocalize with other proteins. The authors also observe CdvB2ΔC localizing to membrane necks by itself (Fig 2E). Therefore, while CdvB1 and CdvB2ΔC colocalize in the flotation assay, there is no strong evidence for CdvB2ΔC recruitment by CdvB1 in dumbbells. This is further underscored by the observation that in the presented data, all Cdv proteins always appear to localize at dumbbell necks, irrespective of what other components are present inside the liposome. Although one nice control is presented (ZipA), this suggests that more work is required to be sure that the proteins are behaving properly in this assay. For example, if membrane binding surfaces of Cdv proteins are mutated, does this lead to the accumulation of proteins in the bulk of the liposome as expected?*

In the particular example of Figure 2I, it indeed appears that there are some clusters of CdvB2ΔC that do not contain CdvB1 (we indicated them in Author response image 3 by red arrowheads), while the yellow arrowheads indicate clusters that contain both proteins. It can be clearly seen that the clusters that do contain both proteins (yellow arrows) are localized at necks, while those that only contain CdvB2ΔC (red arrows) are not localized at necks. This is no coincidence. The clusters indicated by the red arrow do contain CdvB1. However, these clusters rapidly diffuse on the membrane plane because they are not fixed at the neck: therefore, they constantly shift in and out of focus. Because there is a time delay in the acquisition of each channel (between 0.5 and 1 second), these cluster were in focus when the CdvB2ΔC signal was being acquired, but sifted out of focus when the CdvB1 signal was being acquired. This implies that the clusters indicated by the yellow arrowheads are stably localized at necks, which is precisely the point we wished to make with this experiment: because Cdv proteins have an affinity for curved geometry, they preferentially and stably localize at necks. Why don't all the clusters localize at necks then? We estimate that the simple answer is that, in this particular case, there are more clusters than there are necks, so some of the clusters must necessarily localize somewhere else.

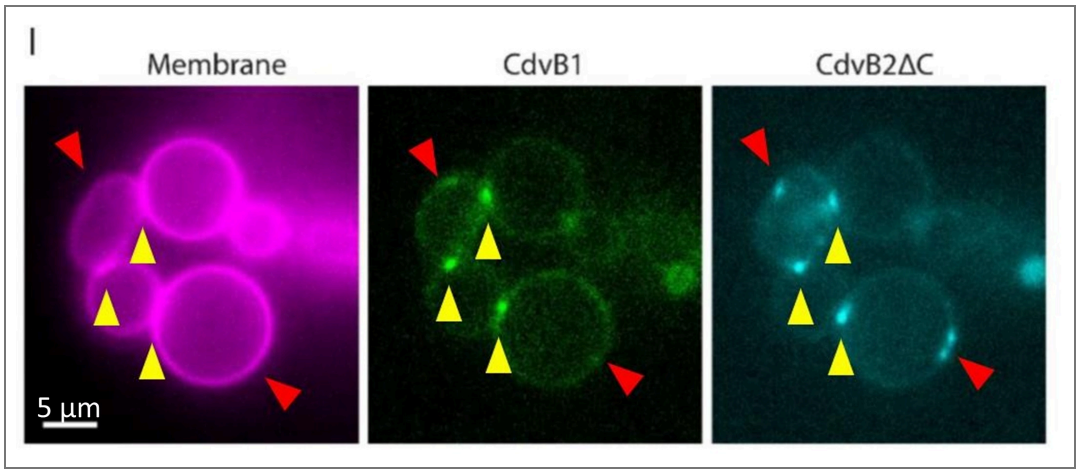

Author response image 3. Current Figure 2H, where clusters that are double-positive for both CdvB1 and CdvB2ΔC are indicated by yellow arrowheads, while cluster that apparently only contain CdvB2ΔC are indicated by red arrowheads. It is observed that all the double-positive clusters are localized at necks.

> *(5) Rings.*
>
> *The authors should comment on why they never observe large Cdv rings in their experiments. In crenarchaeal cell division, CdvA and CdvB have been observed to form large rings in the middle of the 1 micron cell, before constriction. Only in the later stages of division are the ESCRTs localized to the constricting neck, at a time when CdvA is no longer present in the ring. Therefore, if the in vitro assay used by the authors really recapitulated the biology, one would expect to see large CdvAB rings in Figs 1EF. This is ignored in the model. In the proposed model of ring assembly (line 252), CdvAB ring formation is mentioned, but authors do not discuss the fact that they do not observe CdvAB rings - only foci at membrane necks. The discussion section would benefit from the authors commenting on this.*

The referee is correct: it is intriguing that we don't see micron-sized rings for CdvA and CdvB. We do note that our EM data (Fig.S1) show that CdvA in its own can form rings of about 100-200nm diameter, well below the diffraction limit, that could well correspond to the foci that we optically resolve in Figure 1. We now added a brief comment on this to the manuscript on lines 256-264.

> *(6) Stoichiometry*
>
> *It is not clear why 100% of the visible CdvA and 100% of the the visible CdvB are shifted to the lipid fraction in 1C. Perhaps this is a matter of quantification. Can the authors comment on the stoichiometry here?*

We agree that this was unclear. Since that particular gel was stained by coumassie, the quantitative signals might be unreliable, and hence we have repeated this experiment using fluorescently labelled proteins, which show indeed a less extreme distribution. This was also done to make the data more uniform, as requested by the referees.

> *(7) Significance of quantification of MBP-tagged filaments.*
>
> *Authors use tagging and removal of MBP as a convenient, controllable system to trigger polymerisation of various Cdv proteins. However, it is unclear what is the value and significance of reporting the width and length of the short linear filaments that are formed by the MBP-tagged proteins. Presumably they are artefactual assemblies generated by the presence of the tag?*

Providing a measure of the changes induced by MBP removal, in fact, validates that this actually has an effect. But perhaps this places too much emphasis on the short filaments. We now opted for a compromise, removing the quantification of the width and length of short filaments formed by MBPtagged protein from the text, but keeping the supplementary figure showing their distribution as compared to the other filaments (Figure S2E, SF).

> *Similar Figure 2C doesn't seem a useful addition to the paper.*

We removed panel 2C, and now merely report these values in the text.

> ***Recommendations for the authors:***
>
> ***Reviewer #1 (Recommendations for the authors):***
>
> *I would suggest the authors perform a deeper discussion about their findings, such as what are the evolutionary implications, how they think lipids from these archaea may affect the recruitment process,...*

Because there is no exact homology between Archaea Cdv proteins and Eukaryotic ESCRT-III proteins, we do not feel our work brings new evolutionary implications beyond what we already state in the manuscript. We also dis not perform experiments using Archaea lipids, thus we would rather not speculate on how they may potentially affect the recruitment of Cdv proteins.

> *In general, the manuscript lacks information regarding some scale bars, number of experimental repetitions (n or N), statistical analysis when needed, information about protein concentrations used in their assays.*

We have now added this information in the manuscript.

> *Below, I provide a list of comments that I think the authors should address to improve the manuscript:*
>
> *(1) Line 113-114: The authors test protein-membrane interactions using flotation assays with positively curved SUV membranes but encapsulate proteins in dumbbell-shaped liposomes with negative curvature at the connecting necks. Might the use of membranes with opposite curvatures affect the recruitment process? Since the proteins are fluorescently labeled, I suggest testing recruitment using flat giant unilamellar vesicles or supported lipid bilayers (with zero curvature) to validate their findings.*

We thank the referee for this suggestion. Please do note that we are not claiming in our paper that Cdv proteins recognize negative curvature. We merely observe that they localize at necks. The neck of a dumbbell exhibits the so-called “catenoid” geometry, which is characterized by having both positive and negative curvature.

Experimentally, on the SUVs, we now realize there was a mistake in the method section: In the flotation assay we in fact used multilamellar vesicles, not SUVs, precisely for the reason mentioned by the referee. We apologize for the oversight and have now corrected this in the methods. Multilamellar vesicles are not characterized by a strong positive curvature as SUVs do, but we do agree that they likely don’t have negative curvature there either. Because of the heterogeneous nature of the multilamellar vesicles, they provide a binding assay that was rather independent of the curvature. Complementary to the flotation assay, the SMS approach was employed to reveal the curvature preference of proteins.

Finally, we performed the experiment on large GUVs suggested by the referee using CdvB as an example, but this turned out to be inconclusive because the protein forms clusters: these clusters may be creating local curvature at the nanometer scale, which cannot be resolved by

optical microscopy (Author response image 4). This is quite typical for proteins that recognize curvature (cf. for instance: De Franceschi N, Alqabandi M, Miguet N, Caillat C, Mangenot S, Weissenhorn W, Bassereau P. The ESCRT protein CHMP2B acts as a diffusion barrier on reconstituted membrane necks. J Cell Sci. 2018 Aug 3;132(4):jcs217968.)

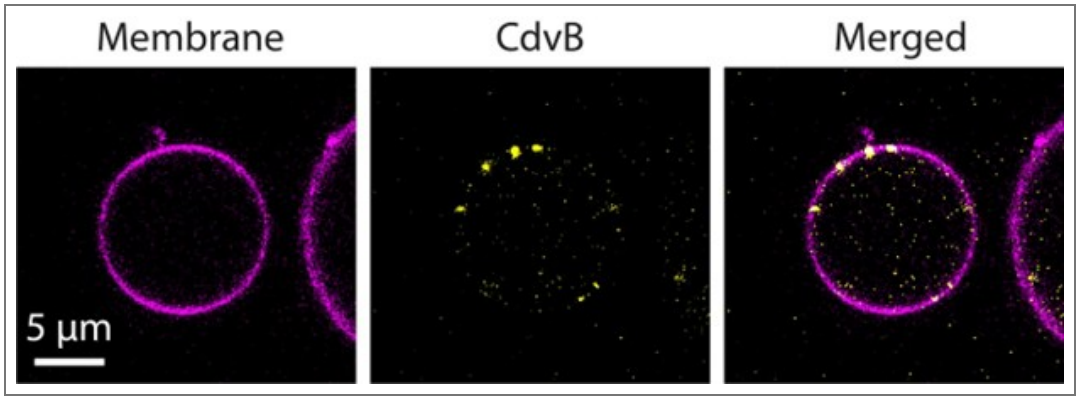

Author response image 4. Fluorescently labelled CdvB bound to giant unilamellar vesicle. The protein was added in the outer buffer. CdvB forms distinct clusters, which may generate a local region of high membrane curvature.

> *(2) Line 138-139: How is His-ZipA binding the membrane? Wouldn't Ni^{2+}-NTA lipids be required? If not, how is the binding achieved?*

Indeed, NTA-lipids were present. This is now stated both in the legend and in the methods.

> *(3) In the encapsulated protein assays, why does the luminal fluorescence intensity of the encapsulated protein sometimes appear similar to the bulk fluorescence signal? Since only a small fraction of the protein assembles at membrane necks, shouldn't the luminal pool of unbound protein show higher fluorescence intensity inside the liposomes?*

We thank the referee for raising this point and giving us the opportunity to explain this. The reason is that Cdv proteins have a very high affinity for the neck, and when they cluster at the neck the fluorescence intensity of the cluster is many times higher than the background fluorescence. Because we were interested in imaging the clusters and avoiding overexposing them, we adjusted the imaging conditions accordingly, with the result that the fluorescence from both the lumen and the bulk is at very low level.

By choosing different imaging conditions, however, it can be actually seen that the signal inside the lumen is clearly higher than the bulk: this can be seen for instance in Author response image 2, where the brightness has been properly adjusted.

> *(4) Line 184-185: In Fig. 2I, some CdvB2ΔC puncta seem independent of CdvB1 and are not localized at membrane necks. How many such puncta exist? For example, in the provided micrograph, 2 out of 5 clusters are independent of CdvB1. This proportion is significant. Could the authors quantify the prevalence of these structures and discuss why they form?*

We thank the referee for giving us the opportunity to explain this apparent discrepancy. We'll like to stress the fact that CdvB2ΔC and CdvB1 form an obligate heterodimer: in all our experiments, without exception, we find that they form a strong complex when we mix the two proteins. This is true both in dumbbells and in flotation assays.

In the particular example of Figure 2I, it indeed appears that there are some clusters of CdvB2ΔC that do not contain CdvB1 (we indicated them in Author response image 3 by red

arrowheads), while the yellow arrowheads indicate clusters that contain both proteins. It can be clearly seen that the clusters that do contain both proteins (yellow arrows) are localized at necks, while those that only contain CdvB2ΔC (red arrows) are not localized at necks. This is no coincidence. The clusters indicated by the red arrow do contain CdvB1. However, these clusters rapidly diffuse on the membrane plane because they are not fixed at the neck: therefore, they constantly shift in and out of focus. Because there is a time delay in the acquisition of each channel (between 0.5 and 1 second), these cluster were in focus when the CdvB2ΔC signal was being acquired, but sifted out of focus when the CdvB1 signal was being acquired. This implies that the clusters indicated by the yellow arrowheads are stably localized at necks, which is precisely the point we wished to make with this experiment: because Cdv proteins have affinity for curved geometry, they preferentially and stably localize at necks. Why don't all the clusters localize at necks then?

> *(5) Figure 1E and 1F: Why do lipids accumulate and colocalize with the proteins? How can the authors confirm lumen connectivity between vesicles? Performing FRAP assays could validate protein localization and enrichment at the lumen of the membrane necks.*

At first sight, indeed some lipid enrichment seems to be observed at the neck between lobes of dumbbells.

This is, however, an imaging artifact due to the fact that the neck is diffraction limited. As shown in the Author response image 5, we are acquiring the membrane signal from both lobes at the neck region, and therefore the signal is roughly double, hence the apparent lipid enrichment.

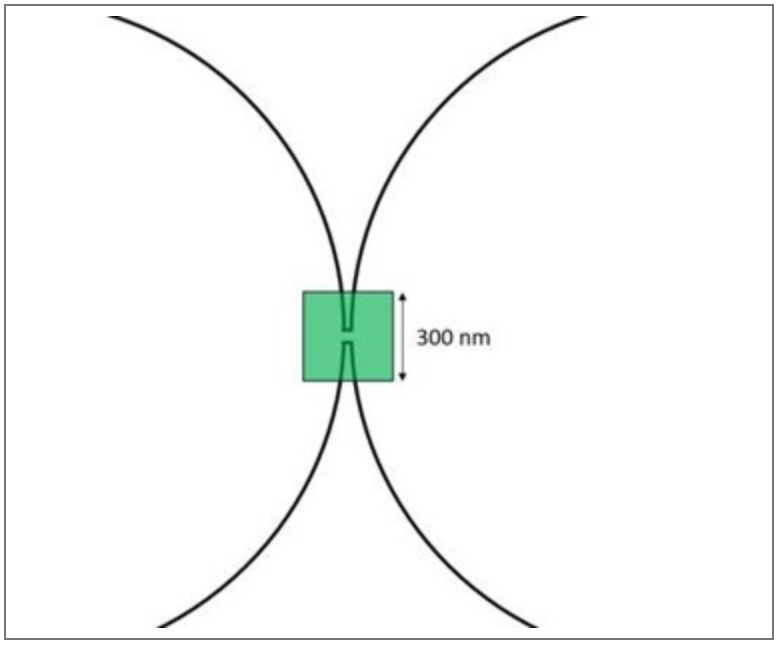

Author response image 5. Schematic illustrating that the neck between two lobes is smaller than the diffraction limit of optical microscopy (the size of a typical pixel is indicated by the green square). Because of this technical limitation, the fluorescence intensity of the membrane at the neck is twice that of a single membrane.

The referee is correct in pointing out that these images do not prove that the lobes are connected, and that FRAP assays is the only way to prove this point. However, in previous papers we have confirmed extensively that in chains of dumbbells the lobes are connected:

- De Franceschi N, Pezeshkian W, Fragasso A, Bruininks BMH, Tsai S, Marrink SJ, Dekker C. Synthetic Membrane Shaper for Controlled Liposome Deformation. ACS Nano. 2022 Nov 28;17(2):966–78. doi: 10.1021/acsnano.2c06125.

- De Franceschi N, Barth R, Meindlhumer S, Fragasso A, Dekker C. Dynamin A as a one-component division machinery for synthetic cells. Nat Nanotechnol. 2024 Jan;19(1):70-76. doi: 10.1038/s41565023-01510-3.

Random sticking of liposomes would also generate clusters of vesicles, not linear chains. We now provide also a Movie (Movie 1) supporting this point.

Investigating whether the necks are open or closed after Cdv reconstitution is indeed a very relevant question, that could be rephrased as “verify whether Cdv proteins or their combination can induce membrane scission”. This is however beyond the scope of this manuscript, as the current work merely addressed the question of hierarchical recruitment of Cdv proteins at the membrane. We plan to examine this in future work.

> *(6) Why didn't the authors use the same lipid composition, particularly the same proportion of negatively charged lipids, on the SUVs of the flotation assays and on the dumbbell-shaped liposomes?*

In flotation assays, it is typical to use a relatively large proportion of negatively charged lipids, to promote protein binding. This is because the aim is to maximize membrane coverage by the protein. The SMS procedure to generate dumbbell-shaped GUVs is completely different, however. Rather than covering the membrane with protein, the idea is to reduce the amount of protein to a minimum, so that any curvature preference can be best visualized. This is e.g. routinely done in tube pulling experiments, for the same reason (See for instance Prévost C, Zhao H, Manzi J, Lemichez E, Lappalainen P, Callan-Jones A, Bassereau P. IRSp53 senses negative membrane curvature and phase separates along membrane tubules. Nat Commun. 2015 Oct 15;6:8529. doi: 10.1038/ncomms9529).

> *(7) Line 117-119: The suggestion that polymer formation between CdvA and CdvB facilitates membrane recruitment is intriguing. However, fluorescence microscopy experiments could better elucidate whether there is sequential recruitment of CdvB followed by CdvA, or if these proteins form a heteropolymer composite for membrane binding. Can CdvB bind membranes independently, or does this require synergy between CdvA and CdvB.*

We thank the referee for prompting us to perform this experiment. As we now show in Figure 1C, CdvB indeed is able to bind the membrane independently of CdvA. Whether this happens sequentially or simultaneously is an interesting question, but one that is impossible to address with either the SMS or the flotation assay, because in both cases we can only observe the endpoint of the recruitment.

We would also like to clarify one specific experimental detail. Perhaps unsurprisingly, the results from the flotation assay are dependent on the way the assay is performed. In particular, we observed that the same protein can exhibit a different binding profile depending on whether it is being loaded either at the top or at the bottom of the gradient. This can be seen in Author response image 6. This is counterintuitive, since once the equilibrium is reached, the result should only depend on the density of the sample. We performed an overnight centrifugation (> 16 hours) on a short tube (< 3 cm tall), thus equilibrium is being reached (which is corroborated by the fact that CdvB1 and CdvB2 can float to the top of the gradient within this timespan, as shown in Figure 2C, 2E, 2G). We ascribe the difference between top and bottom loading to the fact that, when the sample is loaded at the bottom, it has to be mixed with a concentrated sucrose solution, while in the case of loading from the top, this is not done.

In literature, both loading from top and from bottom have been used:

- Lata S, Schoehn G, Jain A, Pires R, Piehler J, Gottlinger HG, Weissenhorn W. Helical structures of ESCRTIII are disassembled by VPS4. Science. 2008 Sep 5;321(5894):1354-7. doi: 10.1126/science.1161070

- Moriscot C, Gribaldo S, Jault JM, Krupovic M, Arnaud J, Jamin M, Schoehn G, Forterre P, Weissenhorn W, Renesto P. Crenarchaeal CdvA forms double-helical filaments containing DNA and interacts with ESCRT-III-like CdvB. PLoS One. 2011;6(7):e21921. doi: 10.1371/journal.pone.0021921.

- Senju Y, Lappalainen P, Zhao H. Liposome Co-sedimentation and Co-flotation Assays to Study LipidProtein Interactions. Methods Mol Biol. 2021;2251:195-204. doi: 10.1007/978-1-0716-1142-5_14. In performing the flotation assay for CdvB1 and CdvB2ΔC, or when using all 4 proteins together, we loaded the sample at the bottom, and we could detect reproducible binding to liposomes (Figures 2D, 2F, 2H, 3A). However, CdvB does not bind the membrane when loaded at the bottom. Thus, for the experiments shown in figure 1C, we loaded the proteins at the top. This experimental setup allowed us to highlight that CdvB indeed induce a stronger interaction between CdvA and the membrane.

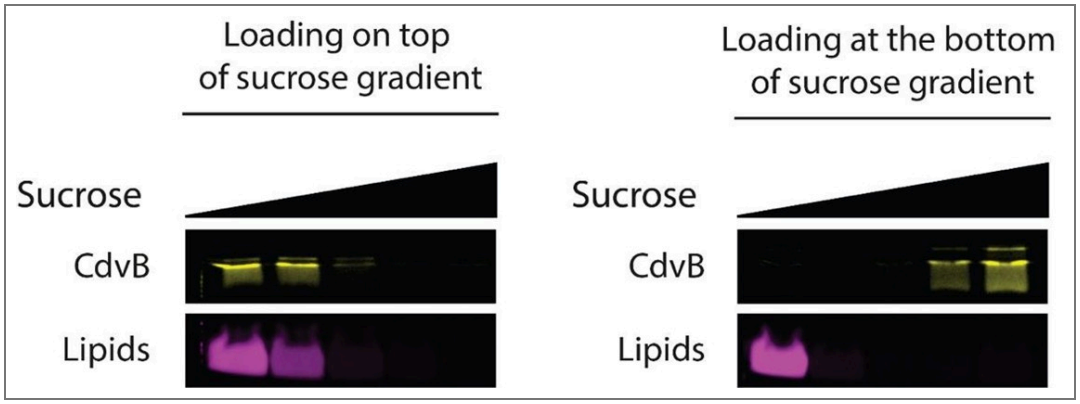

Author response image 6. CdvB binding to multilamellar vesicles in a flotation assay. In the left panel, the sample was loaded at the top of the sucrose gradient; in the right panel it was loaded at the bottom.

> *(8) Line 165-173: The authors claim that filament curvature differs between CdvB2ΔC alone and the CdvB1:CdvB2ΔC complex. Are these differences statistically significant? What is the sample size (N)? Furthermore, how do the authors confirm interactions between these proteins in the absence of membranes based solely on EM micrographs?*

We can confirm that the filaments are composed by both proteins, because the filaments have different curvature when both proteins are present. However, as requested by referee 3, point (7), we removed the quantification of curvature from panel 2C. We report the N number in the text.

> *(9) Line 121-123: Are the authors referring to positive or negative membrane curvatures? The cited literature suggests ESCRT-III proteins either lack curvature preferences (e.g., Snf7, CHMP4B) or prefer high positive curvature (e.g., late ESCRT-III subunits). This is confusing since the authors later test recruitment to negatively curved necks.*

We do not claim that Cdv proteins prefer positive or negative curvature, because the necks present in dumbbells have a catenoid geometry, which include both positive and negative curvature. We have now clarified this in the discussion.

> *(10) Since the conclusions rely on the oligomeric state of the proteins, providing SEC-MALS spectra to show the protein oligomeric state right after the purification would strengthen the claims.*

While such SEC-MALDI experiments may be interesting, practical implementation of this is not possible since both first authors left the lab on to new positions.

> *(11) Line 157-160: Suppl. Fig. 2 shows only a single EM micrograph of a small filament. Could the authors provide lower magnification images showing more filaments?*

As requested by Referee 3, point (7), we have toned down the importance of these short filaments.

> *Also, why are the sample sizes for filament length (N=161) and width (N=129) different?*

Protein filaments formed by Cdv tend to stick to each other side by side, so that for some filaments the width could not be accurately assessed, and accordingly those were removed from the analysis.

> *(12) The introduction states that CdvA binds membranes while CdvB does not. However, the results suggest CdvB facilitates membrane binding, helping CdvA attach. This discrepancy needs further explanation.*

We thank the referee for raising this point. We have now performed additional experiments (both SMS assay and flotation assays) showing that indeed CdvB from *M. sedula* is (unlike CdvB from *Sulfolobus*) able to bind the membrane on its own (Figure 1C, 1F).

> ***Reviewer #2 (Recommendations for the authors):***
>
> *Best practice would be to show single fluorescence channels in grayscale or inverted grayscale, retaining pseudocolouring only for the merged multichannel image.*

We decided to retain and standardize the colors, both for gels and for microscopy images, in order to have the same color-code for each protein. We believe this improves readability, and this was also a request from Referee 3. Thus, throughout the manuscript, CdvA is in grayscale, CdvB in yellow, CdvB1 in green, CdvB2ΔC in cyan and the membrane in magenta.

> *It would be great to include a quantification of liposome curvature vs focal intensity of the various Cdv components - across figures.*

Quantification of liposome curvature at the neck can be done (De Franceschi et al., Nature Nanotech. 2024). However, in practice, this requires transferring of the sample post-preparation into a new chamber in order to increase the signal-to-noise ratio of the encapsulated dye, a procedure that drastically reduces the yield of dumbbells. The very sizeable amount of work required to obtain reliable measurements, especially considering all the proteins and protein combinations used in this study, indicates that this represents a project in itself, which goes well beyond the scope of this manuscript.

> ***Reviewer #3 (Recommendations for the authors):***
>
> *(1) We would encourage the authors to consider including the length of the scale bar next to the scale bar in each image and not in the figure description. This would greatly aid in clarity and interpretation of figures.*

We have now written the length of the scale bar in the figures.

> *(2) In a similar vein, could the authors consider labeling panels throughout the manuscript, writing that sample is being presented? This goes mainly for the negative*

> *stain and the dumbbell fluorescence images, as having to continuously consult the figure legend again hinders clarity.*

We have now labelled the EM images as requested by the referee.

> *(3) Lines 254-256: would the statement hold not only for CdvB2ΔC, but for all imaged proteins? They all seem to localize to membrane necks, presumably favoring membrane binding to a specific membrane topology.*

We agree with the referee, and changed the phrasing accordingly.

> *(4) CdvB2ΔC construct - presumably this was a truncation of helix 5 of the ESCRT-III domain? Figure 1A shows that the ESCRT-III domain spans residues 34-170 and therefore implies that all five ESCRT-III helices (which make up the ESCRT-III domain) are present in the C-terminal truncation. Could the authors clarify?*

Indeed, the truncation was done at residue 170.

(5) Results of the liposome flotation assays are presented inconsistently across the three figures (Figs 1C, 2DFH, and 3A). This makes it more difficult than it needs to be to interpret and compare results. Could the authors consider presenting the three gels in a more similar, standardized way across the three figures?

To improve readability, we now standardized the colors, both for gels and for microscopy images, in order to have the same color-code for each protein. Thus, throughout the manuscript, CdvA is in grayscale, CdvB in yellow, CdvB1 in green, CdvB2ΔC in cyan and the membrane in magenta.

> *(6) From the data presented in Fig 1EF, it cannot be concluded whether CdvB and CdvA colocalize, as only one protein is labelled. Is there a technical reason for this?*

We have now repeated the same experiment by having both proteins labelled, confirming that there is co-localization at the neck (Figure 1G).

> *(7) Fig 2C: is the difference between the two samples significant*

As requested by Referee 3, we have removed Figure 2C.

> *(8) Fig 2I is missing a 'merged' panel.*

We have now added the merged panel.

> *(9) The fluorescence intensity plots in Supp Figs 1C and 3C would be easier to interpret if the lipid and protein signal would be plotted on the same plot (say, with normalized fluorescence intensity)*

It is not immediately obvious to us what the signal should be normalized to. What we wished to convey with these plots was that the intensity of proteins spikes at the neck region. In an attempt to improve clarity, we have now aligned the plots vertically, and highlighted the position of the neck.

> *(10) CdvA should have a capital "A" in Figure 3A, panel 3.*

We have now corrected this.

> *(11) The discussion doesn't comment on the need to truncate CdvB2.*

This is explained in the result session.

https://doi.org/10.7554/eLife.104226.2.sa0